Optimization-Based Islanding of Power Networks Using Piecewise Linear AC Power Flow

Paul A. Trodden, *Member, IEEE*, Waqquas Ahmed Bukhsh, *Student Member, IEEE*, Andreas Grothey, and Ken I. M. McKinnon

***Abstract*—In this paper, a flexible optimization-based framework for intentional islanding is presented. The decision is made of which transmission lines to switch in order to split the network while minimizing disruption, the amount of load shed, or grouping coherent generators. The approach uses a piecewise linear model of AC power flow, which allows the voltage and reactive power to be considered directly when designing the islands. Demonstrations on standard test networks show that solution of the problem provides islands that are balanced in real and reactive power, satisfy AC power flow laws, and have a healthy voltage profile.**

***Index Terms*—Controlled islanding, integer programming, piecewise linear approximation, power system modeling.**

NOMENCLATURE

Sets

$\mathcal{B}$	Buses.
$\mathcal{L}$	Lines.
$\mathcal{G}$	Generators.
$\mathcal{D}$	Loads.
$\mathcal{B}_l$	Buses connected by line l.
$\mathcal{L}_i$	Lines connected to bus i.
$\mathcal{G}_i$	Generators located at bus i.
$\mathcal{D}_i$	Loads located at bus i.
$\mathcal{B}^0$	Buses assigned to section 0.
$\mathcal{B}^1$	Buses assigned to section 1.
$\mathcal{L}^0$	Set of uncertain lines.
$\mathcal{B}^{\mathrm{G}}$	Set of generator buses.

Parameters

$G_i^{\mathrm{B}}, B_i^{\mathrm{B}}$	Shunt conductance, susceptance at bus i.
$g_l, b_l, b_l^{\mathrm{C}}$	Conductance, susceptance, shunt susceptance of line l.
τ_l	Off-nominal tap ratio of line l (if transformer).
V_i^-, V_i^+	Min., max. voltage magnitude at bus i.
$P_g^{\mathrm{G}-}, P_g^{\mathrm{G}+}$	Min., max. real power outputs of generator g.
$Q_g^{\mathrm{G}-}, Q_g^{\mathrm{G}+}$	Min., max. reactive power outputs of generator g.
$P_d^{\mathrm{D}}, Q_d^{\mathrm{D}}$	Real, reactive power demands of load d.
$P_l^{\mathrm{L}+}$	Real power loss limit of line l.
Θ_l, Θ_l^+	Max. angle across l if connected, disconnected.
$c_g(p_g^{\mathrm{G}})$	Generation cost function for generator g.
β_d	Loss penalty for load d.

Variables

v_i, δ_i	Voltage magnitude and phase at bus i.
θ_{ij}	$\delta_i - \delta_j$, voltage phase difference between bus i and j. Note $\theta_{ij} = -\theta_{ji}$.
y_{ij}	$\cos\theta_{ij}$. Note $y_{ij} = y_{ji}$.
z_{ij}	$\sin\theta_{ij}$. Note $z_{ij} = -z_{ij}$.
v_l^i, v_l^j	Voltage magnitudes at either end of line l (which connects buses i and j).
θ_l^{ij}	Voltage phase difference across a line l. Note $\theta_l^{ij} = -\theta_l^{ji}$.
y_l^{ij}	$\cos\theta_l^{ij}$. Note $y_l^{ij} = y_l^{ji}$.
p_l^{ij}, q_l^{ij}	Real, reactive power injection at bus i into line l (which connects buses i and j).
$p_g^{\mathrm{G}}, q_g^{\mathrm{G}}$	Real, reactive power outputs of generator g.
$p_d^{\mathrm{D}}, q_d^{\mathrm{D}}$	Real, reactive power supplied to load d.
α_d	Proportion of load d supplied.
γ_i	Binary. Section (0 or 1) assignment of bus i.
ζ_g	Binary. Connection status of generator g.
ρ_l	Binary. Connection status of line l.

Manuscript received April 15, 2013; revised July 17, 2013, October 01, 2013, and November 15, 2013; accepted November 15, 2013. Date of publication December 18, 2013; date of current version April 16, 2014. This work was supported by the UK Engineering and Physical Sciences Research Council (EPSRC) under grant EP/G060169/1. Paper no. TPWRS-00453-2013.

P. A. Trodden is with the Department of Automatic Control & Systems Engineering, University of Sheffield, Sheffield S1 3JD, U.K. (e-mail: p.trodden@shef.ac.uk).

W. A. Bukhsh, A. Grothey, and K. I. M. McKinnon are with the School of Mathematics, University of Edinburgh, Edinburgh EH9 3JZ, U.K. (e-mail: w.a.bukhsh@sms.ed.ac.uk; a.grothey@ed.ac.uk; k.mckinnon@ed.ac.uk).

Color versions of one or more of the figures in this paper are available online at http://ieeexplore.ieee.org.

Digital Object Identifier 10.1109/TPWRS.2013.2291660

I. INTRODUCTION

THE last decade has seen a number of notable cases of wide-area blackouts as a consequence of severe disturbances and cascading failures [1]–[3]. Although preventive and

corrective systems exist to ameliorate the effects of severe disturbances, the operation of networks closer to limits, together with increased uncertainty in load and distributed generation, means that cascading failures may be harder to prevent, or stop once instigated [4]. Thus, intentional islanding is attracting attention as a corrective measure for limiting the effects of severe disturbances and preventing wide-area blackout.

Intentional islanding aims to split a network, by disconnecting lines, into electrically-isolated islands. The challenge is that, if an island is to be feasible, it must satisfy both static constraints—load/generation balance, network constraints, system limits—and dynamic constraints, *i.e.,* for frequency and voltage stability. Furthermore, the act of islanding must not cause a loss of synchronism or voltage collapse.

The majority of approaches to islanding aim to find, as a primary objective, electromechanically stable islands. A popular approach first uses slow coherency analysis to determine groupings of machines with coherent oscillatory modes, and then aims to split the network along the boundaries of groups [5], [6]. Determining the required cutset of lines involves considerations of load/generation balance, power flows, and other constraints: algorithms include pre-specification of boundaries [7], exhaustive search [5], [6], minimal-flow minimal-cutset determination using a combination of breadth- and depth-first search [8], graph simplification and partitioning [9], spectral clustering [10], and meta-heuristics [11], [12]. A key attraction of the slow-coherence-based approach is that generator groupings are dependent on machine properties and largely independent of fault location and, to a lesser extent, operating point [6]. If the network can be split along the boundaries of these groups, while not causing excessive load/generation imbalance or disruption, the system is less likely to lose stability. Moreover, groupings and line cutsets can be determined offline. Consequently, the online action of islanding is fast, and the approach has been demonstrated effectively by simulations of real scenarios [13], [14].

Another approach uses ordered binary decision diagrams (OBDDs) to determine balanced islands [15]. Subsequently, power flow and transient stability analyses can be used to iterate until feasible, stable islands are found [16]. In [17], a framework is proposed that iteratively identifies the controlling group of machines and the contingencies that most severely impact system stability. A heuristic method is used to search for a splitting strategy that maintains a desired stability margin. Wang *et al.* [18] employed a power flow tracing algorithm to first determine the domain of each generator, *i.e.,* the set of load buses that "belong" to each. Subsequently, the network is coarsely split along domain intersections before refinement of boundaries to minimize imbalances.

While it is known that the sensitivity of coherent machine groupings to fault location is low, it is true that splitting the network along the boundaries of *a-priori* determined coherent groups is not, in general, the only islanding solution that maintains stability. Moreover, such islands may be undesirable in terms of other criteria, such as the amount of load shed, the voltage profile or the possibility that the impacted region may be contained within a larger than necessary island. For example, in [10], the slow-coherence-based islanding of the 39-bus New England system isolates the network's largest generator in an island with no load. In [19], an optimization-based approach to islanding and load shedding was proposed. A key feature is that, unlike many other methods, it can take into account a part of the network that is desired to be isolated—a troublesome area—when determining islands, and isolate this while minimizing the expected amount of load shed or lost. The problem is formulated as a single mixed integer linear programming (MILP) problem, meaning that power balances, flows, and operating limits may be handled explicitly when designing islands, and satisfied in each island in a feasible solution.

The islanding MILP problem has similarities with the *transmission switching* problem [20], in that the decision variables include which lines to disconnect, while power flow constraints must be satisfied following any disconnection. Both approaches—islanding and transmission switching—may be seen as network topology optimization problems with added power flow constraints. In both cases, inclusion of AC power flow laws in the constraints results in a mixed integer nonlinear program (MINLP), which is difficult to solve. Hence, linear DC power flow has been used to date, resulting in a more computationally favorable MILP or MIQP problem.

A disadvantage of the DC power flow model is that the effect of line disconnections on network voltages is not considered. This is not exclusive to MILP-based islanding and transmission switching; a number of islanding approaches consider real power only, and assume that reactive power may be compensated locally after splitting. In [19], however, cases were reported where a solution could not be found to satisfy AC power flow and voltage constraints when the islands were designed considering DC power flow, *even when sufficient reactive power generation capacity was present in each island*. Investigation found that local shortages or surpluses of reactive power led to abnormal voltages in certain areas of the network.

This paper presents a new method for controlled islanding that respects voltage and reactive power constraints. A piecewise linear approximation to AC power flow is developed and then used in a MILP-based approach to islanding: decisions are which lines to disconnect, which loads to shed and how to adjust generators. Results on test networks show this eliminates the AC-infeasibilities reported in [19]. The method is flexible and able to deal with different reasons for islanding. For example, to minimize the load shed while splitting the network so that coherent synchronous machines remain in the same island. Or, to split the network in two so as to ensure that the most of it is left in a known safe state, isolated from a troubled region that has been identified as a possible trigger for cascading failures. The objective would be to minimize the load that is planned to be shed, plus the expected extra load that might be lost due to failures in the small island surrounding the troubled region. There can be many reasons for suspecting trouble from a region—*e.g.,* incomplete or inconsistent measurements, estimates of system stress such as closeness to instability or equipment operating limits, indications of component failures, or other behaviour patterns that simulations have shown to be correlated with cascading failure [21]—but the precise definition of what evidence would lead to islanding being initiated is complex and is beyond the scope of this paper.

The organization of this paper is as follows. In the following section, the piecewise linear AC power flow model is presented,

and its use is demonstrated in an optimal power flow (OPF) problem. In Section III, the islanding formulation is described. Section IV presents computational results for test networks. Conclusions are made in Section V.

II. Piecewise Linear AC Power Flow

A. Linear-Plus-Cosine Model of AC Power Flow

The linear "DC" model is a widely accepted approximation to AC power flow, whose benefits (linearity, simplicity) often outweigh its shortcomings. Recently, however, there has been renewed research interest in the DC model itself [22] and more accurate alternative linearizations [23]. Recent work [19] by the authors found that a DC-based approach to controlled islanding sometimes led to infeasible islands being created, mainly owing to out-of-bound voltages and local shortages or surpluses of reactive power. Motivated by this, this section presents a piecewise linear approximation to AC power flow, in which voltage and reactive power are modeled.

The AC power flow equations are described as follows. Real and reactive power balances at each bus $i \in \mathcal{B}$ give

$$\sum_{g\in\mathcal{G}_i} p_g^{\mathrm{G}} = \sum_{d\in\mathcal{D}_i} p_d^{\mathrm{D}} + \sum_{l\in\mathcal{L}_i, j\in\mathcal{B}_l: j\neq i} p_l^{ij} + G_i^{\mathrm{B}} v_i^2,$$
$$\sum_{g\in\mathcal{G}_i} q_g^{\mathrm{G}} = \sum_{d\in\mathcal{D}_i} q_d^{\mathrm{D}} + \sum_{l\in\mathcal{L}_i, j\in\mathcal{B}_l: j\neq i} q_l^{ij} - B_i^{\mathrm{B}} v_i^2.$$

A line $l \in \mathcal{L}$ connects bus $i \in \mathcal{B}_l$ to bus $j \in \mathcal{B}_l, j \neq i$. The power flows from i to j are

$$p_l^{ij} = v_i^2 G_l^{ii} + G_l^{ij} v_i v_j y_{ij} + B_l^{ij} v_i v_j z_{ij},$$
$$q_l^{ij} = -v_i^2 B_l^{ii} - B_l^{ij} v_i v_j y_{ij} + G_l^{ij} v_i v_j z_{ij},$$

with a similar expression from j to i, where

$$\tau_l^2 G_l^{ii} = G_l^{jj} = -\tau_l G_l^{ij} = -\tau_l G_l^{ji} = g_l,$$
$$\tau_l^2 B_l^{ii} = B_l^{jj} = b_l + 0.5 b_l^{\mathrm{C}},$$
$$-\tau_l B_l^{ij} = -\tau_l B_l^{ji} = b_l.$$

The convention is for a transformer to be located at the *from* end (bus i) of a branch.

The standard "DC" approximation to AC power flow linearizes these equations by using the approximations $v_i = v_j = 1$, $z_{ij} = \theta_{ij}$, $y_{ij} = 1$, and $b_l \gg g_l \approx 0$ yielding $p_l^{ij} = B_l^{ij}\theta_{ij}$. The reactive power variables and equations are dropped. In the model in this paper, voltage and reactive power are retained. Expanding the line flows about $v_i = 1$, $v_j = 1$ and $\theta_{ij} = 0$ (hence $y_{ij} = 1, z_{ij} = 0$):

$$p_l^{ij} \approx G_l^{ii}(2v_i - 1) + G_l^{ij}(v_i + v_j + y_{ij} - 2) + B_l^{ij} z_{ij},$$
$$q_l^{ij} \approx B_l^{ii}(1 - 2v_i) - B_l^{ij}(v_i + v_j + y_{ij} - 2) + G_l^{ij} z_{ij}.$$

In a standard linearization, the small-angle approximations would then be used: $y_{ij} = \cos\theta_{ij} \approx 1$ and $z_{ij} = \sin\theta_{ij} \approx \theta_{ij}$.Table I gives the maximum absolute errors for each of the constituent terms in the linearized flows, over a typical range of operating voltages and angles, *i.e.,* $0.95 \leq v_i \leq 1.05$ at each end of the line, and $|\theta_{ij}| \leq 40°$. The cosine approximation incurs the largest error. Fig. 1 shows maximum and minimum power flows and errors over this range of voltages and angles for a line with $g_l = 1, b_l = -5, b_l^{\mathrm{C}} = 1$. Approximation errors are obtained for when the $y_{ij} = \cos\theta_{ij}$ term is approximated as 1 (a linear model) and modeled exactly (linear plus cosine). In both cases, $z_{ij} = \theta_{ij} \approx \sin\theta_{ij}$ is used. Although little reduction in errors is apparent in the real flows, the importance of modeling the cosine term is clear for reactive flows.

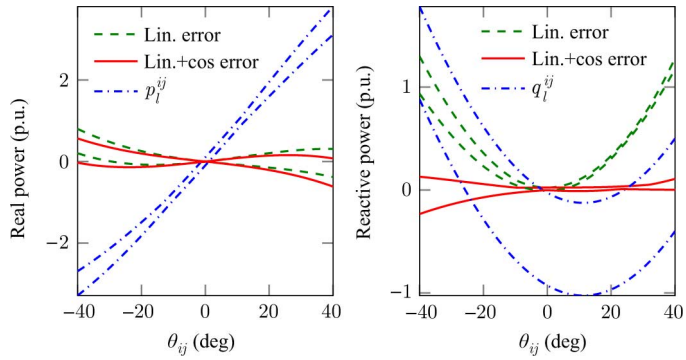

Fig. 1. Maxima and minima of power flows, and of approximation errors, as a function of phase angle difference.

TABLE I
Approximation Errors in Line Flow Terms (Voltages in P.U.)

Term	Approximation	Max abs error
v_i^2	$2v_i - 1$	0.0025
$v_i v_j y_{ij}$	$v_i + v_i + y_{ij} - 2$	0.0253
$v_i v_j z_{ij}$	z_{ij}	0.0659
y_{ij}	1	0.2340
z_{ij}	θ_{ij}	0.0553

A similar analysis shows that including the sine term (instead of its linearization) in addition to the cosine term reduces the error in the real flows slightly, but makes no significant difference to the reactive power. Since the infeasibilities that occur using the DC approach to islanding are mainly owing to the reactive power and voltage limits [19], the appropriate approximation to use is the linear-plus-cosine one. And although cosine terms cannot be used directly in an MILP model, they can be modeled to arbitrary levels of accuracy by piecewise linear functions. The next section demonstrates the use of the model in an OPF formulation.

B. Piecewise Linear AC OPF

The piecewise linear (PWL) AC OPF problem is defined as

$$\min \sum_{g\in\mathcal{G}} c_g\left(p_g^{\mathrm{G}}\right)$$

subject to, $\forall i \in \mathcal{B}$, the linearized power balances:

$$\sum_{g\in\mathcal{G}_i} p_g^{\mathrm{G}} = \sum_{d\in\mathcal{D}_i} P_d^{\mathrm{D}} + \sum_{l\in\mathcal{L}_i, j\in\mathcal{B}_l: j\neq i} p_l^{ij} + G_i^{\mathrm{B}}(2v_i - 1), \quad (1a)$$
$$\sum_{g\in\mathcal{G}_i} q_g^{\mathrm{G}} = \sum_{d\in\mathcal{D}_i} Q_d^{\mathrm{D}} + \sum_{l\in\mathcal{L}_i, j\in\mathcal{B}_l: j\neq i} q_l^{ij} - B_i^{\mathrm{B}}(2v_i - 1). \quad (1b)$$

Line flows for all $l \in \mathcal{L}, i, j \in \mathcal{B}_l : i \neq j$:

$$p_l^{ij} = G_l^{ii}(2v_i - 1) + G_l^{ij}(v_i + v_j + y_{ij} - 2) + B_l^{ij}\theta_{ij},$$
$$q_l^{ij} = B_l^{ii}(1 - 2v_i) - B_l^{ij}(v_i + v_j + y_{ij} - 2) + G_l^{ij}\theta_{ij}.$$

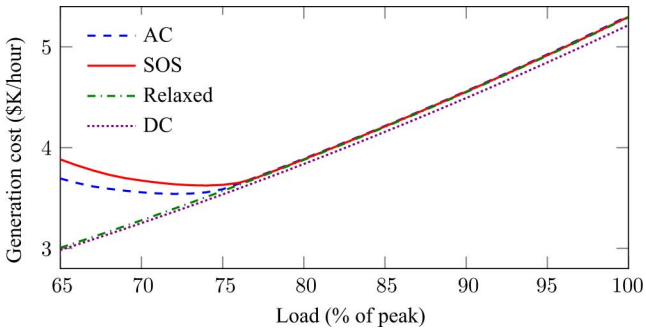

Fig. 2. Generation costs as a function of load for the 9-bus network.

The N-piece PWL approximation to $\cos\theta_{ij}$. For all $l \in \mathcal{L}, i, j \in \mathcal{B}_l : i \neq j$:

$$y_{ij} = h_{ij,k}\theta_{ij} + d_{ij,k}, \forall \theta_{ij} \in [x_{ij,k}, x_{ij,k+1}], k = 0 \ldots N-1 \tag{2}$$

where $h_{ij,k}$ and $d_{ij,k}$ are chosen so that the approximation coincides with $\cos x$ at breakpoints $\{x_{ij,0}, \ldots, x_{ij,N}\}$. System limits are applied:

$$\begin{aligned} V_i^- &\leq v_i \leq V_i^+, \forall i \in \mathcal{B}, \\ P_g^{\mathrm{G}-} &\leq p_g^{\mathrm{G}} \leq P_g^{\mathrm{G}+}, \forall g \in \mathcal{G}, \\ Q_g^{\mathrm{G}-} &\leq q_g^{\mathrm{G}} \leq Q_g^{\mathrm{G}+}, \forall g \in \mathcal{G}, \\ p_l^{ij} + p_l^{ji} &\leq P_l^{\mathrm{L}+}, \forall l \in \mathcal{L}. \end{aligned} \tag{3}$$

Note that line flow limits are limits on real power (I^2R) loss. If an MVA limit $S_l^{\mathrm{L}+}$ is given, this may be converted by assuming nominal voltage, *i.e.*, $P_l^{\mathrm{L}+} = (g_l/g_l^2 + b_l^2)\left(S_l^{\mathrm{L}+}\right)^2$.

The implementation (2) of the PWL model of $\cos\theta_{ij}$ requires either binary variables or special ordered sets of type 2 (SOS-2) [24]. The overall problem is then, depending on c_g, a mixed integer linear or quadratic program (MILP or MIQP). If (2) is replaced by its relaxation $y_{ij} \leq h_{ij,k}\theta_{ij} + d_{ij,k}$, then the problem becomes a convex optimization problem and no binary variables or SOS sets are needed. Since real and reactive line losses decrease as y_{ij} increases, it is tempting to assume that equality will hold for one of the PWL sections, and this relaxation will yield a tight result. However, as Fig. 2 shows, situations exist where the SOS formulation is necessary. This shows optimal generation costs against load level, as obtained by OPFs using AC, PWL with SOS, relaxed PWL, and DC power flow models. The network is the WSCC 9-bus network modified to set voltage limits to $\pm 5\%$ and the lower reactive power limit for each generator is raised from -300 to -5 Mvar. This means that at low load levels the generators find it increasingly difficult to balance the reactive power, as more lines become sources rather than sinks of reactive power, and the generation cost rises with falling load. While the SOS PWL is able to capture this effect, the relaxed PWL and DC-based models are not; the former "cheats" by having some lines continue to store reactive power irrespective of their end voltages and angles—allowed because $y_{ij} < h_{ij,k}\theta_{ij} + d_{ij,k}$ is permitted—and this allows more of the real power to be generated by the cheaper generators.

III. Formulation for System Islanding Using Piecewise Linear AC Power Flow

In [19], the problem of determining how to split a transmission network into islands is considered. The aim is to limit the effects of possible cascading failures and prevent the onset of wide-area blackouts by re-configuring the network—*via* line switching—so that problem areas are isolated. The MILP-based method defines two *sections* of the network. All of the buses that must be isolated are pre-assigned to section 0, and the optimization determines which other buses and lines to place in section 0. All the remaining components are in section 1. This creates at least two islands. The optimization will also determine the best strategy to adjust generation and shed load so as to establish a load-generation balance in each island while respecting all network equations and operating constraints after the split.

A. Motivation: Effect of Topology Changes on Voltage Profile

Solution of the MILP islanding problem provides a set of lines to switch, loads to shed and generators to adjust. However, if only the DC power flow equations are included in the constraints, the effects of changing the network topology on voltages and reactive power flows is not considered. Thus, in [19], an AC optimal load shedding (OLS) problem is solved *after* the MILP islanding problem, using the islanded network topology. If a solution to this can be found, the islanded network is feasible with respect to AC power flow and operating constraints. The solution provides the correct generator output and load adjustments to make, now having considered voltage and reactive power.

However, a number of the islanding solutions in [19] were AC infeasible, primarily due to violation of voltage bounds; solutions could be recovered by relaxing the normal limits. One such example, for the 24-bus IEEE Reliability Test System (RTS) [25], is described as follows. Given the problem of isolating bus 6 while minimizing the expected load shed or lost, the optimal solution islands buses 1, 2 and 6, as indicated in Fig. 3. There remains sufficient real power capacity in both islands to meet demand, and no load is shed. Moreover, but not by design, there is sufficient reactive power capacity in each island to meet the total reactive power demand. Despite this, a feasible solution to the AC-OLS cannot be found. Softening the voltage bounds recovers a solution, but with an abnormally low voltage of 0.6443 p.u. at bus 6 and an over-limit flow on line (2,6). Further inspection reveals that this situation has arisen because of the disconnection of line (6,10), a cable with high shunt capacitance. The passive shunt reactor at bus 6 would, in normal circumstances, balance locally the excess reactive power and maintain a satisfactory voltage profile. This problem could be avoided by linking together the disconnection of line (6,10) and the shunt reactor at 6. The optimal solution when these actions are linked is shown in the right-hand diagram of Fig. 3, and it yields a better feasible solution than when the reactor is not disconnected. Rules like this are easy to incorporate in the model; however, it is difficult *a-priori* to define all possible rules. A better approach is to allow the model to decide the combination of equipment to disconnect, and when this is done the optimal solution disconnects both line (6,10) and the reactor at bus 6, giving the right-hand Fig. 3 solution. The models and result for this example are given in Sections III-B4 and IV-A1.

This is just one example of where an islanding solution formed by considering only real power—even if network

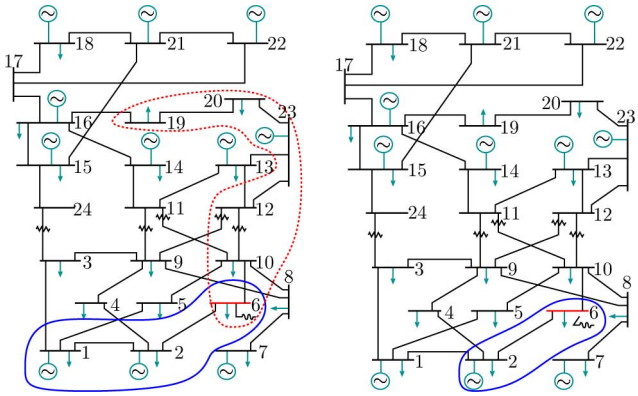

Fig. 3. IEEE 24-bus RTS with bus 6 isolated. On the left, DC method (solid) and PWL method without shunt switching (dashed). On the right, PWL method with shunt switching.

constraints are included—is unsatisfactory. It also shows that even if reactive power balance is achieved within each island, local shortages or surpluses can lead to an abnormal voltage profile. Many test networks are prone to this problem [19]. Moreover, it is not just system islanding that is susceptible; DC-based transmission switching also does not consider the consequences on voltage of disconnecting lines. Thus, there is a need for network topology optimization methods that can determine AC-feasible solutions, but without having to resort to solving the full MINLP problem. The focus of this paper is topology optimization for the purpose of islanding, and in the next section, a formulation is presented that uses the PWL model of AC power flow.

B. Formulation of Constraints for Islanding

The problem is to decide which lines to switch in order to isolate a part of the network. Separation of sections is enforced by sectioning constraints. The islanded network must satisfy power balance and flow equations and operating limits, and so these are included as constraints in the problem.

1) Sectioning Constraints: Define $\mathcal{B}^0$ and $\mathcal{B}^1$, where $\mathcal{B}^0 \cap \mathcal{B}^1 = \emptyset$, as the subsets of buses that are desired to be separated. For now, the motivation for this separation is left open, but it may be that these buses in, say, $\mathcal{B}^0$ represent a failing area of the network, or are associated with a coherent group of synchronous machines that will be separated from other groups. The proposed approach will split the network into two *sections*: section 0 will contain all buses in $\mathcal{B}^0$ and section 1 all buses in $\mathcal{B}^1$. For a bus $i \in \mathcal{B}$, γ_i denotes the section (0 or 1) to which that bus is assigned. That is, if i is to be placed in section 0, then $\gamma_i = 0$. Separation between sections is achieved by switching lines: ρ_l denotes the connection status of a line l, and the convention followed is for $\rho_l = 0$ when l is disconnected. The exact boundaries of each section will depend on the objective, defined later, and the optimization will determine how to assign to sections those buses not in $\mathcal{B}^0$ or $\mathcal{B}^1$, in order achieve balance and optimize the objective. However, the following constraints enforce the separation of section 0 and 1, without predefining their boundaries:

$$\rho_l \le 1 + \gamma_i - \gamma_j, \forall l \in \mathcal{L}, i, j \in \mathcal{B}_l : i \ne j, \tag{4a}$$

$$\gamma_i = s, \forall i \in \mathcal{B}^s, s \in \{0, 1\}. \tag{4b}$$

2) Power Flow: The remainder of the constraints are concerned with achieving a balanced steady state for the islanded network. It is assumed that generators are permitted to make only small-scale changes to output or be switched off, and loads may be fully or partly shed in order to maintain a balance. As a consequence of these changes and the topological changes, bus voltages, angles and line flows will change, and so must be modeled to ensure satisfaction of network constraints and operating limits.

First, the power balances, (1a) and (1b), are included without modification. Next, the line flow equations are modified so that when a line is disconnected, power flows across it are zero irrespective of its end bus voltages and angles. To assist this, we introduce *line* variables—v_l^i and v_l^j as end voltages and θ_l^{ij} as the angle difference—that are distinct from *bus* variables v_i, v_j and θ_{ij}. The following constraints control the relationship between line variables and bus variables. For a line $l \in \mathcal{L}$ with end buses i and j

$$-\Theta_l \rho_l \le \theta_l^{ij} \le \Theta_l \rho_l, \tag{5a}$$

$$-\Theta_l^+(1-\rho_l) \le \theta_l^{ij} - \theta_{ij} \le \Theta_l^+(1-\rho_l), \tag{5b}$$

$\forall i \in \mathcal{B}_l$:

$$0 \le v_i - v_l^i \le (V_i^+ - V_i^-)(1-\rho_l), \tag{5c}$$

$$V_i^- \le v_l^i \le V_i^- + (V_i^+ - V_i^-)\rho_l, \tag{5d}$$

and $\forall i \in \mathcal{B}$,

$$V_i^- \le v_i \le V_i^+, \tag{5e}$$

where $\Theta_l^+ \ge \Theta_l$ is a "big-M" constant. Of these, (5a) and(5b) force equality of θ_l^{ij} and $\theta_{ij} = \delta_i - \delta_{ij}$ for a connected line, but set $\theta_l^{ij} = 0$ for a disconnected line while allowing the *bus* angles δ_i and δ_j to vary independently. Likewise, if $\rho_l = 1$ then, by (5c), $v_l^i = v_i$ and $v_l^j = v_j$. However, if $\rho_l = 0$ then the line voltages are set to minimum values—$v_l^i = V_i^-$ and $v_l^j = V_j^-$—independent of the bus voltages v_i and v_j.

This switching between line and bus variables is made use of in modified line flow equations. For a line l

$$p_l^{ij} = G_l^{ii}(2v_l^i - 1) + G_l^{ij}\left(v_l^i + v_l^j + y_l^{ij} - 2\right) + B_l^{ij}\theta_l^{ij} - \left(G_l^{ii}(2V_i^- - 1) + G_l^{ij}(V_i^- + V_j^- - 1)\right)(1-\rho_l), \tag{6a}$$

$$q_l^{ij} = B_l^{ii}(1 - 2v_l^i) - B_l^{ij}\left(v_l^i + v_l^j + y_l^{ij} - 2\right) + G_l^{ij}\theta_l^{ij} - \left(B_l^{ii}(1 - 2V_i^-) - B_l^{ij}(V_i^- + V_j^- - 1)\right)(1-\rho_l) \tag{6b}$$

and y_l^{ij} is given by (2), using θ_l^{ij}. Note that since $\theta_l^{ij} = 0$ if $\rho_l = 0$, then $y_l^{ij} = 1$ for a disconnected line. Hence, if $\rho_l = 0$ then $p_l^{ij} = 0$, irrespective of v_i, v_j and $\theta_{ij} = \delta_i - \delta_j$. If $\rho_l = 1$, the normal power flow equations are recovered.

3) Operating Constraints: In the short time available when islanding in response to a contingency, any extra generation that is needed will be achieved by a combination of the ramping-up of online units and the commitment of fast-start units. For simplicity, fast-start units are not considered in the examples in this paper. We assume that a generator that is operating can either have its input mechanical power disconnected, in which case real output power drops to zero in steady state, or its output can be set to a new value within a small interval, $\left[P_g^{G-}, P_g^{G+}\right]$, say,

for generator g, around the pre-islanded value. The limits will depend on the ramp and output limits of the generator, and the amount of immediate or short-term reserve capacity available to the generator. For the test scenarios in Section IV, a time limit of 2 min is assumed for ramping, but the formulation permits any choice. This choice should be informed by existing post-contingency response protocols. For reactive power, it is assumed that a new output can be set in some range $Q_g^{\mathrm{G}-}$ to $Q_g^{\mathrm{G}+}$. The set of possible real and reactive power outputs of a generator is usually convex. For the test scenarios in Section IV, the bounds on the real and reactive power are independent. In the more general case, since the range of values for the real power output is small, the feasible region for the problem is a narrow slice through a convex set, and—except when the real power output is close to its upper limit—it is a good approximation to treat the real and reactive power bounds as independent. If this is not the case, it is straightforward to add constraints that couple p_g^{G} and q_g^{G}.

The operating regime is modeled by the constraints

$$\zeta_g P_g^{\mathrm{G}-} \leq p_g^{\mathrm{G}} \leq \zeta_g P_g^{\mathrm{G}+}, \forall g \in \mathcal{G}, \tag{7a}$$

$$Q_g^{\mathrm{G}-} \leq q_g^{\mathrm{G}} \leq Q_g^{\mathrm{G}+}, \forall g \in \mathcal{G}, \tag{7b}$$

$$\zeta_g = 1, \forall g \in \left\{\mathcal{G} : P_g^{\mathrm{G}-} = 0\right\} \cup \mathcal{G}^1. \tag{7c}$$

Here, ζ_g is a binary variable and denotes the on/off setting of the real power output, and $\mathcal{G}^1$ is a subset of generators which are required to remain on.

For loads, because of the limits on generator outputs and network constraints, it may not be possible after islanding to fully supply all loads. It is therefore assumed that some shedding of loads is permissible. Note that this is *intentional* shedding, not automatic shedding as a result of low voltages or frequency. To implement this in the real network there has to be central control over equipment. For all $d \in \mathcal{D}$

$$p_d^{\mathrm{D}} = \alpha_d P_d^{\mathrm{D}}, \tag{8a}$$

$$q_d^{\mathrm{D}} = \alpha_d Q_d^{\mathrm{D}} \tag{8b}$$

where $0 \leq \alpha_d \leq 1$.

Finally, line limits are applied via constraint (3).

4) Rules for Other Component Switching: As motivated by Section III-A, sometimes it is necessary to have rules for switching components or adjusting controls in different situations. Such rules can easily be included in the formulation using standard techniques for deriving constraints from logical rules [26]. For example, the switching of a shunt component at a bus i can be modeled by introducing binary and continuous variables, ξ_i and u_i respectively, constraints

$$\xi_i(2V_i^- - 1) \leq u_i \leq \xi_i(2V_i^+ - 1),$$
$$-(1-\xi_i)(2V_i^- - 1) \leq u_i - (2v_i - 1) \leq (1-\xi_i)(2V_i^+ - 1)$$

and replacing the $G_i^{\mathrm{B}}(2v_i - 1)$, $B_i^{\mathrm{B}}(2v_i - 1)$ terms in (1a) and (1b) with $G_i^{\mathrm{B}} u_i$ and $B_i^{\mathrm{B}} u_i$, respectively. In Section IV-A1 this is explored further for the 24-bus example.

C. Objective Functions for Islanding

The general aim is to split the network, separating the two sections 0 and 1, yet leaving it in a feasible state of operation. The specific motivations and objectives for islanding are discussed in this section. Clearly, if a network can be partitioned with minimal disruption to load, and with minimal disturbances to generators, then its chances of viable operation until future restoration are increased.

1) Isolating Uncertain Regions and Maximizing Expected Load Supply: We assume that there is an identifiable localized area of the network that is believed could be a trigger for cascading failure. Similar to the approach in [19], the goal is to include this area of potential trouble in an island, leaving the rest of the network in a known, secure steady state. The sets $\mathcal{B}^0$ and $\mathcal{L}^0$ consist of all buses and lines in the troubled area and, additionally, any buses and lines whose status is uncertain. To ensure section 1 contains no uncertain components, all lines $l \in \mathcal{L}^0$ remaining in this section are disconnected by replacing (4a) by

$$\rho_l \leq 1 - \gamma_i, \forall i \in \mathcal{B}_l. \tag{9}$$

Because section 0 may contain failing components or be in an uncertain state, it is assumed there is a risk of not being able to supply any load placed in that section. Accordingly, a load loss penalty $0 \leq \beta_d < 1$ is defined for a load d, which may be interpreted as the probability of being able to supply a load if placed in section 0. Suppose a reward R_d is obtained per unit supply of load d. If d is placed in section 1 a reward R_d is realized per unit supply; however, if d is placed in section 0, a lower reward of $\beta_d R_d < R_d$ is realized.

The objective is then to maximize the expected total value of load supplied:

$$J^{\mathrm{exp\,load}} = \sum_{d \in \mathcal{D}} R_d P_d^{\mathrm{D}} (\beta_d \alpha_{0d} + \alpha_{1d}) \tag{10}$$

where $\alpha_d = \alpha_{0d} + \alpha_{1d}$, and $0 \leq \alpha_{1d} \leq \gamma_b, \forall b \in \mathcal{B}, d \in \mathcal{D}_b$. Here a new variable α_{sd} is introduced for the load d delivered in section $s \in \{0, 1\}$. If $\gamma_b = 0$ (and so the load at bus b is in section 0), then $\alpha_{1d} = 0$, $\alpha_{0d} = \alpha_d$, and the reward is $\beta_d R_d P_d^{\mathrm{D}} \alpha_d$. Conversely, if $\gamma_b = 1$ then $\alpha_{1d} = \alpha_d$ and $\alpha_{0d} = 0$, giving a larger reward $R_d P_d^{\mathrm{D}} \alpha_d$. Thus, maximizing (10) gives a preference for $\gamma_b = 1$ and a smaller section 0, so that the impacted area is limited.

2) Promoting Generator Coherency: Another aim is to ensure the synchronicity of generators within islands. Large disturbances in the network cause electro-mechanical oscillations, which can lead to a loss of synchronism. A popular approach is to split the system along boundaries of near-coherent generator groups, as determined by slow-coherency analysis [27]. Thus, weak connections between machines—which give rise to slow, lightly-damped oscillations—are cut, leaving separate networks of tightly-coupled, coherent machines.

Consider those buses in the network with generators attached, the set of which is defined as $\mathcal{B}^{\mathrm{G}}$, and define $\mathcal{B}^{\mathrm{GG}} \triangleq \left\{(i,j) \in \mathcal{B}^{\mathrm{G}} \times \mathcal{B}^{\mathrm{G}} : j > i\right\}$ as the set of all pairs of such buses. For what follows, it may be assumed that multiple units at a bus are tightly coupled and are aggregated to a single unit. The dynamic coupling, W_{ij}, between a pair of machines at buses $(i,j) \in \mathcal{B}^{\mathrm{GG}}$ may be determined from slow-coherency analysis. For example, assuming as in [10] the undamped second order swing equation

$$W_{ij} = \frac{\partial(\dot{\omega}_i - \dot{\omega}_j)}{(\delta_i - \delta_j)} = \left(\frac{1}{M_i} + \frac{1}{M_j}\right) \frac{\partial P_{ij}}{\partial \delta_{ij}}$$

where M_i, ω_i, δ_i are the inertia constant, angular frequency and rotor angle of the machine at bus i, and $\partial P_{ij}/\partial \delta_{ij}$ is the synchronizing power coefficient or "stiffness" between machines

at i and j. To favour, in the objective, separating loosely-coupled generators, introduce a new variable $0 \leq \eta_{ij} \leq 1$ for all $(i,j) \in \mathcal{B}^{\mathrm{GG}}$. Then the constraint

$$-\eta_{ij} \leq \gamma_i - \gamma_j \leq \eta_{ij} \tag{11}$$

sets η_{ij} to 1 if generator buses i and j are in different sections of the network (and hence electrically isolated), but otherwise may be zero. Minimizing the function

$$J^{\mathrm{coh}} = \sum_{(i,j)\in\mathcal{B}^{\mathrm{GG}}} W_{ij}\eta_{ij} \tag{12}$$

gives a preference for machines in different sections having small W_{ij}, *i.e.,* being weakly coupled, and those within the same section have stronger coupling. This may be used in conjunction with (10), *i.e.,* $\max J^{\exp\,\mathrm{load}} - kJ^{\mathrm{coh}}$, with weighting $k > 0$, so that section 0 is the "unhealthy" section, and the expected load supply is maximized while keeping together strongly-coupled machines.

Minimizing (12) alone will favour keeping all machines in the same section, and to force the machines apart additional constraints may be needed. Alternatively, the following implementation splits the network directly into coherent groups, making different use of the sets $\mathcal{B}^0$ and $\mathcal{B}^1$.

3) Splitting Into Coherent Groups: Suppose that coherent groups of generators have been determined, and that assigned to $\mathcal{B}^0$ and $\mathcal{B}^1$ are those buses in $\mathcal{B}^{\mathrm{G}}$ corresponding to machines in different groups. For example, $\mathcal{B}^0$ may contain the critical coherent group of machines, and $\mathcal{B}^1$ all others. The sectioning constraints will ensure that the machines are separated, but which other buses are assigned to each section is determined by the optimization. The solution that minimizes the amount of load shed can be found by maximizing the function

$$J^{\mathrm{load}} = \sum_{d\in\mathcal{D}} \alpha_d P_d^{\mathrm{D}}. \tag{13}$$

Alternatively, to seek a solution that changes the generator outputs minimally from their initial values P_g^{G0}, minimize

$$J^{\mathrm{gen}} = \sum_{g\in\mathcal{G}} t_g \tag{14}$$

where $t_g \geq 0, t_g \geq p_g^{\mathrm{G}} - P_g^{\mathrm{G0}}$, and $t_g \geq -p_g^{\mathrm{G}} + P_g^{\mathrm{G0}}, \forall g \in \mathcal{G}$. The sectioning constraints ensure that the machines are split into two sections. If further separation is required, the optimization can be re-run on each island of the network.

4) Penalties: Often there may be multiple feasible solutions with objective values close to the optimum. Including additional penalty terms in the objective—small enough to not significantly affect the primary objective—improves computation by encouraging binary variables to take integral values in the relaxations, and also guides the solution process towards particular solutions. For example, consider the penalty terms (for a minimization problem)

$$\sum_{l\in\mathcal{L}} W^y(1-y_l) + \sum_{l\in\mathcal{L}} W_l^{\mathrm{L}}(1-\rho_l) + \sum_{g\in\mathcal{G}} W_g^{\mathrm{G}}(1-\zeta_l) \tag{15}$$

where W^y, W_l^{L}, W_g^{G} are weights to be chosen appropriately. The first term penalizes line losses, and reduces the need for SOS branching. The second penalizes cutting lines. We found these substantially reduced the number of lines that are cut beyond those needed to create the island, and this significantly improved solution times. Also, if W_l^{L} is set to a small multiple of the pre-islanding power flow through the line, disconnecting high-flow lines is penalized most heavily; in [19] it was shown that this leads more often to solutions that retain dynamic stability. The third term penalizes the switching-off of generators. If $W_g^{\mathrm{G}} = \epsilon P_g^{\mathrm{G}+}$ then units are given uniform weighting. If, say, $W_g^{\mathrm{G}} = \epsilon \left(P_g^{\mathrm{G}+}\right)^2$, then the disconnection of large units is discouraged.

D. Overall Formulation

The overall problem is to optimize the chosen islanding objective [*e.g.,* (10), (12), (13), or (14)], subject to

- sectioning constraints (4);
- line switching constraints (5);
- power balance [(1a) and (1b)] and flow (6) constraints;
- the PWL approximation (2);
- generation limits (7);
- line flow limits (3);
- load shedding constraints (8).

IV. Computational Results

A. Islanding to Minimize Expected Load Loss

A set of scenarios was built based on the 9-, 14-, 24-, 30-, 39-, 57-, 118-, and 300-bus test systems from MATPOWER [28]. For a network with n^{B} buses, n^{B} scenarios were generated by assigning in turn each single bus to $\mathcal{B}^0$. No buses were included in $\mathcal{B}^1$ and no lines in $\mathcal{L}^0$. For each scenario, the islanding solution was obtained by solving the previously described MILP problem. The feasibility of an islanding solution was checked by solving an AC optimal load shedding (OLS) problem on the islanded network, which includes all AC power balance, flow and operating constraints, but permits load shedding as per (8a) and (8b).

Data for the islanding problems are described as follows. In the objective function, $J^{\exp\,\mathrm{load}}$, a value of 0.75 is used for the load loss penalty β_d. The generator coherency objective, J^{coh}, was not included initially. The penalties are $W_g^{\mathrm{G}} = 0.01P_g^{\mathrm{G}+}$, $W^y = 0.1$ and $W_l^{\mathrm{L}} = 0.0025\sum_d P_d^{\mathrm{D}}$, so that the line-cut penalty is scaled by the total load in the system. Our investigations show that these penalties have a negligible effect (0.2%) on the quality of the solutions, but reduce computation time by an order of magnitude. For the PWL approximation for a line l, first the angle difference prior to islanding, θ_l^*, is determined from the base-case AC OPF solution, and then 12 pieces are used over $\pm(|\theta_l^*| + 10^\circ)$.

Operating limits, including voltage and line limits, were obtained from each network's data file [28]. Generator real power output limits ($P_g^{\mathrm{G}-}$ and $P_g^{\mathrm{G}+}$) were set, as explained in Section III-B3, to allow a 2-min ramp change from the current output P_g^{G0}, where ramp rates were available in the network data, or a 5% change where they were not. In either case, the output limits were limited by capacity limits. P_g^{G0} was obtained by solving an AC OPF on the intact network prior to islanding. Then in the islanding problem, the lower limit was raised by 5% of $(P_g^{\mathrm{G}-} - P_g^{\mathrm{G}+})$. The post-islanding AC OLS, however, was permitted to use the full range, $[P_g^{\mathrm{G}-}, P_g^{\mathrm{G}+}]$. This avoids those solutions where an island is infeasible because of too much generated real power.

TABLE II
24-BUS SYSTEM: COMPARISON OF SOLUTIONS

Solution	DC	PWL-AC-1	PWL-AC-2
MILP islanding solution			
$J^{\text{exp load}}$ (MW)	2764.8	2679.2	2753.8
Generation (MW)	2850.0	2892.7	2844.1
Exp. load shed (MW)	85.3	170.8	96.2
Post-islanding AC-OLS			
$J^{\text{exp load}}$ (MW)	$\star$	2671.2	2753.2
Generation (MW)	$\star$	2884.4	2847.8
Exp. load shed (MW)	$\star$	178.9	96.8

1) AC-Feasible Islanding of 24-Bus Network: Returning to the example of Section III-A, the PWL AC islanding approach is applied to the problem of islanding bus 6. The islanding problem was solved both with and without the option (as part of the optimization) of switching the shunt reactor at bus 6. The optimal solutions are shown in Fig. 3. Without shunt switching (PWL-AC-1), the cable (6,10) is left intact and the final network topology is significantly different from before. With shunt switching permitted (PWL-AC-2), the cable is again switched, but fewer buses are islanded than for the DC solution. The feasibility of each solution was checked by solving the AC OLS problem on the islanded network, and both PWL AC solutions satisfied all AC constraints.Table II compares the DC, PWL-AC-1 and PWL-AC-2 solutions, using values obtained from both the MILP solutions and the post-islanding AC solutions. The PWL AC islanding solutions are close to the final AC OLS solutions. Note that the PWL AC solutions achieve AC feasibility at the cost of a lower expected load supply (hence higher expected load shed).

2) Computation Time: The speed with which islanding decisions have to be made depends on whether the decision is being made before a fault has occurred, as part of contingency planning within secure OPF, or after, in which case the time scale depends on the cause of the contingency. Finding solutions that are optimal, or to within a pre-specified percentage of optimality, can take an unpredictable amount of time. Hence, especially in the latter case of reacting after a fault has occurred, it is important to be able to produce good feasible solutions within short time periods even if these are not necessarily optimal. To illustrate how the quality of the solution depends on the solution time, tests were run for a set of fixed times of between 5 and 45 s, returning the best found integer feasible solution.Table III summarizes these results for the 57-, 118-, and 300-bus scenarios, quoting the average relative MIP gap of returned solutions. All the test cases with 39 or fewer buses solved to negligible % gaps within 5 s, and are not shown.Table III also shows the average gaps between the returned and best-known AC solutions for each scenario, where an AC solution was obtained from a returned PWL islanding solution by solving the AC-OLS on the islanded network. The mean error between the objectives of the returned PWL-AC and AC solutions was less than 0.02%. For each network and scenario, the best-known AC solution was the best from those found from the different termination times, plus longer 1000-s runs. In the second and third sections of Table III, the mean values are over all cases that were feasible within the time limit. The platform was a 64-bit Dual Intel Xeon processor and 128 GiB RAM with up to 12 threads and using CPLEX 12.5 as the MILP solver.

TABLE III
SOLUTIONS TO ISLANDING PROBLEMS FOR DIFFERENT TIME LIMITS

Time (s)	5	10	15	20	30	45
Percentage with no islanding solution found within time						
57-bus	1.7	0.0	0.0	0.0	0.0	0.0
118-bus	0.0	0.0	0.0	0.0	0.0	0.0
300-bus	17.7	7.7	3.0	0.7	0.0	0.0
Mean % between best MIP solution and the MIP bound						
57-bus	0.04	0.31	0.21	0.13	0.13	0.08
118-bus	0.43	0.13	0.08	0.05	0.04	0.03
300-bus	0.08	0.15	0.11	0.18	0.14	0.05
Mean % between best AC solution found in time and best known						
57-bus	0.19	0.14	0.12	0.06	0.06	0.05
118-bus	0.23	0.09	0.12	0.04	0.04	0.04
300-bus	0.03	0.09	0.07	0.12	0.11	0.06

TABLE IV
COHERENCY-BASED ISLANDING OF 39-BUS NETWORK

	Section 0	Section 1
Buses	1–3, 5–9, 30, 31, 39	4, 10–29, 32–38
Generation (MW)	2007.18	3992.29
Load supplied (MW)	1997.89	3945.37
Load shed (MW)	297.21	13.76

The results show that good islanding solutions were found within 30 s —and usually sooner—for all networks. Moreover, the islanding topology usually changes little, or not at all, between the solutions returned at 5 s and 45 s.

3) AC Feasibility: Using the DC model 20% of cases led to AC-infeasible islands [19], whereas none of the islands found using the PWL AC model were infeasible.

4) Promoting Generator Coherency: The generator coherency objective, J^{coh}, may be included for the 24-bus network example by taking second-order dynamic data taken from [25]. For example, when $\mathcal{B}^0 = 3$, maximizing just $J^{\text{exp load}}$ leads to an optimal solution that places bus 1 in section 0 along with bus 3, and an expected load supply of 2699 MW. In doing this, the line between buses 1 and 2 is switched, separating the large generator sets at these buses (which would incur a cost of $J^{\text{coh}} = 2.26$). However, when maximizing the joint objective with $k = 100$, the optimal solution does not include bus 1 in section 0, opting instead to leave the line (1,2) intact and placing just buses 3 and 9 in section 0. With $k = 100$, the expected load supply is slightly smaller (2670 MW), but the strongly-coupled generators at buses 1 and 2 remain connected ($J^{\text{coh}} = 0.00$).

B. Coherency-Based Islanding

The coherency-based splitting approach was applied to the 10-machine, 39-bus New England test network. Slow coherency analysis, assuming second-order dynamics, shows that the machines may be divided into two groups: those at buses 30, 31 and 39 in one group, and then all others.

With $\mathcal{B}^0 = \{30, 31, 39\}$ and $\mathcal{B}^1 = \mathcal{B}^{\text{G}} \setminus \mathcal{B}^0$, the optimal solution splits the system as shown in Table IV. Note that although buses 1–3 and 5–9 are included in the same section as 30, 31, and 39, no generators are present at these buses. The objective was to minimize the movement of generator real power outputs, *i.e.,* (14). To achieve this split and leave the islands balanced, the generator at bus 32 has to lower its output from 671 to 373 MW, while 311 MW is shed. It is worth stating that no other solution

exists that splits these two groups but requires less total change in generator outputs.

V. Conclusions and Future Work

An optimization-based framework for the intentional or controlled islanding of power networks has been presented. The approach is flexible with respect to the aims and objectives of islanding, and finds islands that are balanced and satisfy real and reactive power flow and operating constraints. It has been shown that the inclusion of a piecewise linear model of AC power flow allows AC-feasible islands to be found, where previously a DC-based approach led to islands with out-of-bound voltages. The use of objectives that promote generator coherency has been demonstrated.

Future work will investigate the wider practical aspects of the approach by performing detailed simulations on representative networks and blackout scenarios, considering transient and dynamic performance. Current work is exploring the use of decomposition and aggregation methods to improve the computational efficiency for larger networks.

References

[1] Final Report of the Investigation Committee on the 28 September 2003 Blackout in Italy, Union for the Coordination of the Transmission of Electricity (UCTE), Final Report, 2004.

[2] U.S.-Canada Power System Outage Task Force, Final Report on the August 14 2003 Blackout in the United States and Canada: Causes and Recommendations, Final Report. Apr. 2004 [Online]. Available: https://reports.energy.gov/

[3] S. Larsson and A. Danell, "The black-out in southern Sweden and eastern Denmark," in *Proc. IEEE Power Syst. Conf. Expo., 2006*, Sep. 23, 2003.

[4] J. W. Bialek, "Lights out?," *IEE Power Engineer*, vol. 19, p. 16, 2005.

[5] H. You, V. Vittal, and Z. Yang, "Self-healing in power systems: An approach using islanding and rate of frequency decline-based load shedding," *IEEE Trans. Power Syst.*, vol. 18, no. 1, pp. 174–181, Feb. 2003.

[6] H. You, V. Vittal, and X. Wang, "Slow coherency-based islanding," *IEEE Trans. Power Syst.*, vol. 19, no. 1, pp. 483–491, Feb. 2004.

[7] S. S. Ahmed, N. C. Sarker, A. B. Khairuddin, M. R. B. A. Ghani, and H. Ahmed, "A scheme for controlled islanding to prevent subsequent blackout," *IEEE Trans. Power Syst.*, vol. 18, no. 1, pp. 136–143, Feb. 2003.

[8] X. Wang and V. Vittal, "System islanding using minimal cutsets with minimum net flow," in *Proc. IEEE Power Syst. Conf. Expo.*, 2004.

[9] G. Xu and V. Vittal, "Slow coherency based cutset determination algorithm for large power systems," *IEEE Trans. Power Syst.*, vol. 25, no. 2, pp. 877–884, May 2010.

[10] L. Ding, F. M. Gonzalez-Longatt, P. Wall, and V. Terzija, "Two-step spectral clustering controlled islanding algorithm," *IEEE Trans. Power Syst.*, vol. 28, no. 1, pp. 75–84, Feb. 2013.

[11] L. Liu, W. Liu, D. A. Cartes, and I.-Y. Chung, "Slow coherency and angle modulated particle swarm optimization based islanding of large-scale power systems," *Adv. Eng. Informat.*, vol. 23, no. 1, pp. 45–56, 2009.

[12] M. R. Aghamohammadi and A. Shahmohammadi, "Intentional islanding using a new algorithm based on ant search mechanism," *Int. J. Elect. Power Energy Syst.*, vol. 35, pp. 138–147, 2012.

[13] B. Yang, V. Vittal, G. T. Heydt, and A. Sen, "A novel slow coherency based graph theoretic islanding strategy," in *Proc. IEEE Power Eng. Soc. General Meeting*, 2007.

[14] G. Xu, V. Vittal, A. Meklin, and J. E. Thalman, "Controlled islanding demonstrations on the WECC system," *IEEE Trans. Power Syst.*, vol. 26, no. 1, pp. 334–343, Feb. 2011.

[15] K. Sun, D.-Z. Zheng, and Q. Lu, "Splitting strategies for islanding operation of large-scale power systems using OBDD-based methods," *IEEE Trans. Power Syst.*, vol. 18, pp. 912–923, 2003.

[16] K. Sun, D. Z. Zheng, and Q. Lu, "Searching for feasible splitting strategies of controlled system islanding," *IEE Proc. Gen., Transm., Distrib.*, vol. 153, pp. 89–98, 2006.

[17] M. Jin, T. S. Sidhu, and K. Sun, "A new system splitting scheme based on the unified stability control framework," *IEEE Trans. Power Syst.*, vol. 22, no. 1, pp. 433–441, Feb. 2007.

[18] C. G. Wang, B. H. Zhang, Z. G. Hao, J. Shu, P. Li, and Z. Q. Bo, "A novel real-time searching method for power system splitting boundary," *IEEE Trans. Power Syst.*, vol. 25, pp. 1902–1909, 2010.

[19] P. A. Trodden, W. A. Bukhsh, A. Grothey, and K. I. M. McKinnon, "MILP formulation for controlled islanding of power networks," *Int. J. Elect. Power Energy Syst.*, vol. 45, no. 1, pp. 501–508, 2013.

[20] E. B. Fisher, R. P. O'Neill, and M. C. Ferris, "Optimal transmission switching," *IEEE Trans. Power Syst.*, vol. 23, no. 3, pp. 1346–1355, Aug. 2008.

[21] M. Vaiman, K. Bell, Y. Chen, B. Chowdhury, I. Dobson, P. Hines, M. P. S. Miller, and P. Zhang, "Risk assessment of cascading outages: Methodologies and challenges," *IEEE Trans. Power Syst.*, vol. 27, pp. 631–641, 2012.

[22] B. Stott, J. Jardim, and O. Alsaç, "DC power flow revisited," *IEEE Trans. Power Syst.*, vol. 24, pp. 1290–1300, 2009.

[23] C. Coffrin, P. V. Hentenryck, and R. Bent, "Approximating line losses and apparent power in AC power flow linearizations," in *Proc. 2012 IEEE Power & Energy Soc. General Meeting*, 2012.

[24] E. M. L. Beale and J. J. H. Forrest, "Global optimization using special ordered sets," *Math. Program.*, vol. 10, pp. 52–69, 1976.

[25] Reliability Test System Task Force of the Application of Probability Methods Subcommittee, "IEEE reliability test system—1996," *, IEEE Trans. Power Syst.*, vol. 14, no. 3, pp. 1010–1020, Aug. 1999.

[26] H. P. Williams*, Logic and Integer Programming*, ser. International Series in Operations Research & Management Science. New York, NY, USA: Springer, 2009.

[27] B. Avramovic, P. K. Kokotovic, J. R. Winkelman, and J. H. Chow, "Area decomposition for electromechnical models of power systems," *Automatica*, vol. 16, pp. 637–648, 1980.

[28] R. D. Zimmerman, C. E. Murillo-Sánchez, and R. J. Thomas, "MATPOWER Steady-State Operations, Planning and Analysis Tools for Power Systems Research and Education," *IEEE Trans. Power Syst.*, vol. 26, no. 1, pp. 12–19, Feb. 2011.

Paul A. Trodden (S'06–M'09) received the M.Eng. degree in engineering science from the University of Oxford, U.K., in 2003, and the Ph.D. degree in aerospace engineering from the University of Bristol, U.K., in 2009.

He is a lecturer in the Department of Automatic Control and Systems Engineering, University of Sheffield, U.K. His research interests include robust and predictive control, distributed control, and optimization for power systems.

Waqquas Ahmed Bukhsh (S'13) received the B.S. degree in mathematics from COMSATS University, Islamabad, in 2008. He is currently pursuing the Ph.D. degree in the School of Mathematics at the University of Edinburgh, U.K.

Andreas Grothey received the M.Sc. degree in numerical analysis from the University of Dundee, U.K., in 1995 and the Ph.D. degree in optimization from the University of Edinburgh, U.K., in 2001.

He is a senior lecturer in the School of Mathematics at the University of Edinburgh. His interests include algorithms for stochastic and other large scale optimization problems with applications to optimal power flow.

Ken I. M. McKinnon received the B.Sc. degree in mathematics and physics from the University of Glasgow, U.K., and the Ph.D. degree in optimization from the Control Engineering Department at Cambridge University, U.K.

He is the Professor of operational research in the School of Mathematics at the University of Edinburgh, U.K. His current research interests are in structure exploiting numerical optimization methods and their application to energy systems.